Photodarkening Measurements in Large-Mode-Area Fibers

Joona Koponen[a], Mikko Söderlund[a], Hanna J. Hoffman[a], Dahv Kliner[b], and Jeffrey Koplow[b]
[a]Liekki Corporation, Sorronrinne 9, FI-08500 Lohja, Finland
[b]Sandia National Laboratories, Livermore, CA, USA

ABSTRACT

Yb-doped fibers are widely used in applications requiring high average output powers and high power pulse amplification. Photodarkening is one limiting factor in these fibers. In this paper, characterization of photodarkening in large-mode-area (LMA) fibers is presented building upon our previous work, which indicated that meaningful comparison of photodarkening properties from different fibers can be made as long as care is taken to equalize the excited state Yb concentration between samples. We have developed a methodology that allows rapid and reproducible photodarkening measurements to be performed and that enables quantitative comparison of the photodarkening propensity among fibers with different compositions and under different operating conditions. We have shown that this measurement technique can be used effectively for LMA fibers by employing cladding pumping rather than the more standard core pumping. Finally, we observe a seventh-order dependence of the initial photodarkening rate on the excited-state Yb population for two different Yb-doped fibers; this result implies that photodarkening of a Yb-doped fiber source fabricated using a particular fiber will be strongly dependent on the device configuration.

Keywords: photodarkening, ytterbium, fiber laser, fiber amplifier

1. INTRODUCTION

Ytterbium (Yb)-doped fiber lasers and amplifiers have become an attractive option for generating light in the 1.04-1.1µm wavelength region. Double-clad fiber sources have become increasingly popular because of the high output beam quality and brightness, the possibility to use low brightness pump sources, and the high surface-area-to-volume ratio, which facilitates removal of the heat generated in the fiber.[1] The output powers of Yb-doped double-clad fibers have steadily increased over the past few years, rising to the kW level, and fiber lasers and amplifiers have progressed from research laboratories to commercially available devices.[2-6] High-power devices are often realized with large-mode-area (LMA) fibers (i.e., large core diameter and low numerical aperture). LMA fibers are of interest because the resultant decrease in irradiance at a given power level (or decrease in fluence at a given pulse energy) increases the threshold for undesirable nonlinear processes and for optical damage. In addition, the length of the doped fiber may be considerably shortened by increasing the core/cladding area ratio and/or by increasing the Yb concentration, which results in higher pump absorption. For many applications, shortening the length of the Yb-doped fiber is highly beneficial, for example, in reducing nonlinearities in high-peak-power amplifiers. On the other hand, higher concentrations and/or higher pumping rates have been known to result in deleterious effects, the most troublesome of which is the phenomenon of photodarkening (PD), generally acknowledged as a process that can potentially limit both the efficiency and the lifetime of Yb-doped fiber devices. Such PD, attributed to the formation of optically induced structural changes in the glass, is commonly manifested as a time-dependent broadband absorption at visible and near-IR wavelengths. Reduction, or preferably elimination, of this damage mechanism would greatly enhance the prospects for development and fielding of practical fiber lasers and amplifiers in applications requiring predictable performance in hands-free, long-term operational settings. To achieve this goal, meaningful characterization tools, as well as better understanding of the PD phenomenon, must be developed.

Photodarkening of rare-earth doped fibers has been reported for many different glasses doped with, for example, Tm^{3+}, Ce^{3+}, Pr^{3+}, Eu^{2+}, and Yb^{3+}.[7-10] The PD can be attributed to the formation of color centers or other light-induced structural deformations in the doped glass core.[11] While most of the excess loss is induced at visible wavelengths, a significant amount of PD may also be present at the near-IR signal and pump wavelengths. The PD process is driven largely by the energy of signal and pump photons causing optical losses in the doped core only; the process is thus distinguishable from other detrimental effects, such as polymer coating damage or glass radiation damage from high-energy particles.

Previously we have observed that for many silica glass compositions, the spectral shape of the induced excess loss is constant, which means that by measuring the excess loss at a visible wavelength, namely 633 nm, we can calculate the excess loss at the signal wavelength.[12] We also observed that the initial PD rate for a given Yb-doped fiber depends on the degree of inversion, and that this rate is independent of pump power at a given inversion level.[13] Different applications, such as a CW laser or a pulsed amplifier, induce different inversion levels in the fiber, and the same fiber will thus photodarken faster or slower depending on the application.

In this study we present two approaches to induce a flat and reproducible inversion profile in Yb-doped fiber samples of various dimensions, from single-mode to LMA. The parameters affecting the initial PD rate (as observed during the first hours and days of the process) are discussed, and suitable parameters for different measurement methods are suggested. Additionally, we have taken a systematic approach to produce a flat and tunable inversion in an Yb-doped fiber sample, and we have measured the PD rate at different inversion levels. These results support our hypothesis that the level of inversion is the main controlling parameter for initial PD rate.

2. PHOTODARKENING OF LMA FIBERS

Photodarkening measurements can be realized either by measuring the properties of a small sample of the doped fiber of interest, or by creating a full fiber laser or amplifier system where the total efficiency and output power are measured as a function of time. For benchmarking different Yb-doped fibers a fast, quantitative, and repeatable method is preferred. The methodology, measurement approaches, and main parameters for such benchmarking methods are presented below. The benchmarking methods are based on our observation that inversion is the main parameter affecting the rate of PD.

LMA fibers are used in both high power cw lasers and in high-peak-power amplifiers. Therefore the range of inversion levels in the fibers vary over a broad range, and the PD behavior of the fiber changes from application to application. To further complicate the characterization of PD in specific applications, there is the possibility that the induced excess loss may be annealed, for example, by subjecting fibers to elevated temperatures for a period of time, as has recently been pointed out.[14] Thus, in high-power applications (or any application where the fiber is exposed to temperatures significantly higher than room temperature), the final level of PD may be defined by the equilibrium state of two competing processes: progression and annealing of PD. Whether a final steady state is reached and at what power level will therefore depend on the nature of the operating conditions. A standardized measurement technique that can be applied to a variety of pumping conditions and required performance levels would therefore be of great practical interest, both to the manufacturers and the users of fibers. The benchmarking methods presented here are for the study of the initial photodarkening rate of both single-mode and LMA fibers, and by the use of these methods a head-to-head comparison of the PD susceptibility of different fibers can be implemented.

2.1 Benchmarking methods

The measurement technique we proposed for benchmarking single-mode Yb-doped fibers relies on saturating the inversion of the fiber to a flat and repeatable level across the sample by core pumping the sample with a high-intensity, single-mode, fiber-coupled pump.[12] With this technique, PD can be measured with either a monochromatic or a white-light source coupled into the core of the fiber. As the area of the fiber core increases, the inversion becomes harder to saturate using a single-mode pump diode, and other means of inducing the flat and repeatable inversion level in the fiber sample must be introduced. Such means include cladding pumping of a short fiber sample, but the typical pump intensity is several orders of magnitude lower than with core pumping, and the inversion is thus difficult to saturate. The measurement setups are illustrated in Fig. 1 for both the core-pumping and cladding-pumping methods. The PD measurement consists of measuring the transmission of the sample fiber before and after exposure to pump light, either by measuring a probe signal with a power meter or a white-light source with an optical spectrum analyzer. During PD of the sample, care should be taken to insure that the sample is not lasing, as any lasing significantly decreases the inversion level. Signal light feedback should be prevented by, for example, using angled fiber ends.

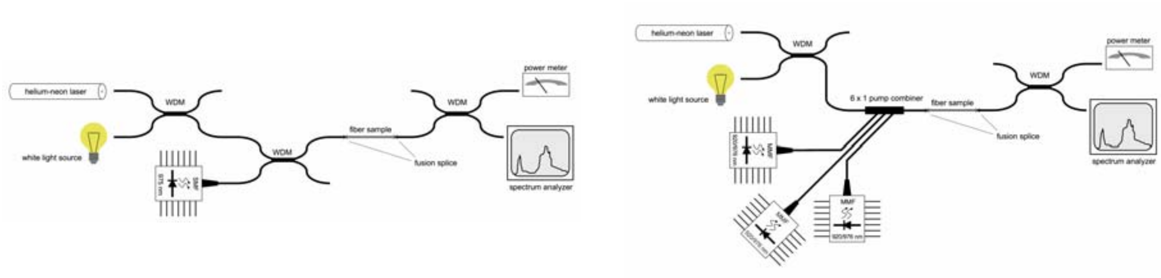

(a) (b)

Fig. 1. (a) Core-pumping method for benchmarking. Single-mode laser diode is coupled to the sample fiber using a wavelength division multiplexer (WDM). Either a probe laser, for example HeNe, or a white-light source can be used to measure the transmission of sample before, after, or during PD. (b) Cladding-pumping method uses a multimode combiner (MMC) to couple light from multimode laser diodes to the sample fiber. By using a multimode combiner equipped with a signal fiber, the probe laser or other light source can be coupled to the core of the sample fiber.

2.2 Measurement parameters

To decrease the time required for each measurement the inversion in the fiber sample must be maximized during the measurement in order to rapidly induce PD. On the other hand the inversion level needs to be reproducible between measurements. Inversion of a fiber sample is defined by the pump brightness, the sample properties, and the pump wavelength, and the most convenient way of deriving the inversion profile of the fiber is by simulation. The results presented here were calculated using commercially available fiber simulation software, Liekki Application Designer v3.0. For simulating fiber types of different compositions, the absorption and emission cross-section data need to be updated accordingly in order to calculate the inversion correctly. Simulation parameters used within this section are 10 cm sample length, variable core diameter, Yb^{3+} ion density of 1.2×10^{26} m^{-3}, and excited-state lifetime of 0.85 ms. The pump wavelength was varied between 920 nm and 976 nm.

The inversion profile of a core-pumped sample was simulated as a function of pump power (Fig. 2). The average inversion over the whole sample and the standard deviation of the inversion were calculated. The inversion was presumed to be sufficiently flat when the standard deviation was less than 1% over the sample length. Figure 2 illustrates how a core-pumped sample inversion saturates, after which the level of inversion is defined by the ratio of absorption and emission cross sections at the pump wavelength. The attainable inversion at 920 nm pump wavelength is higher than at 976 nm due to the lower emission cross section at 920 nm.

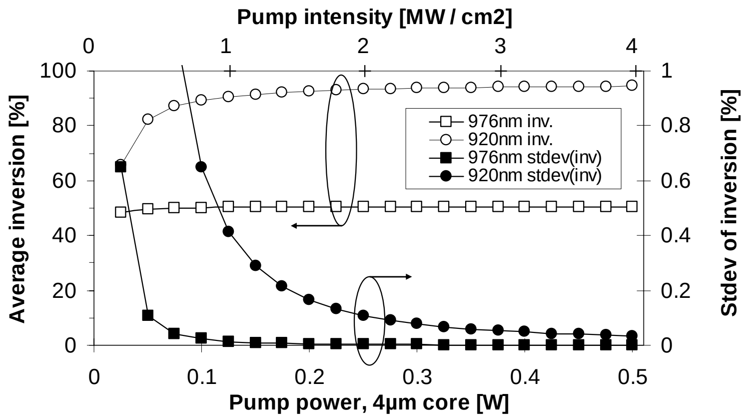

Fig. 2. Average inversion and standard deviation of the inversion vs. pump power for a core-pumped, Yb-doped fiber. The inversion of the sample saturates, i.e. additional pump power no longer increases the inversion. The saturated inversion level is mainly defined by the ratio of absorption and emission cross sections.

The core-pumping method using a single-mode, fiber-coupled, high-brightness diode relies on inversion saturation to achieve inversion flatness and repeatability between different samples. With increasing core size, as is the case with LMA fibers, at some point the fiber sample can no longer be saturated using reasonable pump power, and the inversion over the fiber sample is no longer flat and repeatable. From previous calculations, the threshold levels for saturation using 920 nm and 976 nm pumping were approximately 1200 kW/cm^2 and 300 kW/cm^2, respectively. Figure 3 shows the required pump power as a function of core diameter for these irradiances. Presuming a single-mode, fiber-coupled pump with 500 mW output power, the maximum core diameters feasible for inversion saturation using core pumping are approximately 7 µm and 14 µm for 920 nm and 976 nm pumping, respectively. In practical measurement setups, one should operate further away from the calculated limits due to, for example, coupling losses.

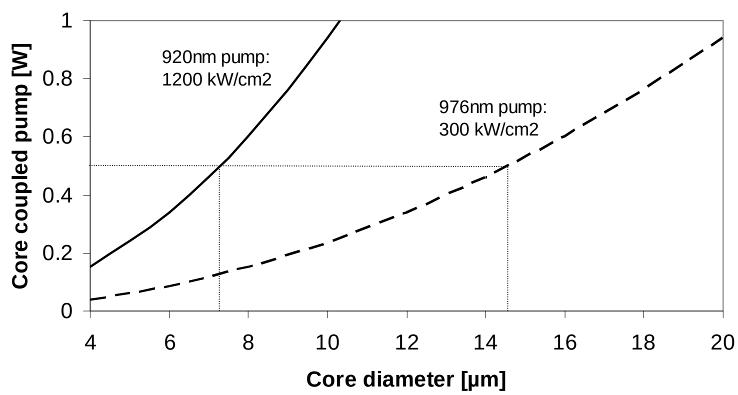

Fig. 3. Maximum saturated core diameter for 920 nm pump wavelength and 0.5 W pump power is approximately 7 µm presuming the 1200kW/cm^2 requirement for pump irradiance. For 976 nm pumping, the irradiance of 300 kW/cm^2 is reached at approximately 14 µm when using 0.5 W of pump power.

To accommodate the needs of >14 µm core diameter fibers, a different method of inducing a flat and repeatable inversion is required. Cladding pumping using multimode pump diodes, as illustrated in Fig. 1(b), fulfills the requirements. Figure 4 shows the calculated average level and standard deviation of the inversion over a fiber sample with a 20 µm core diameter and 400 µm cladding diameter. The results indicate that a flat (<1% standard deviation) inversion is achieved over the whole range of pump power, but the average inversion achieved is a function of pump power. The operational regime is far from the intensity thresholds for inversion saturation; 1200 kW/cm^2 for a 400 µm diameter fiber translates to approximately 1.5 kW of pump power.

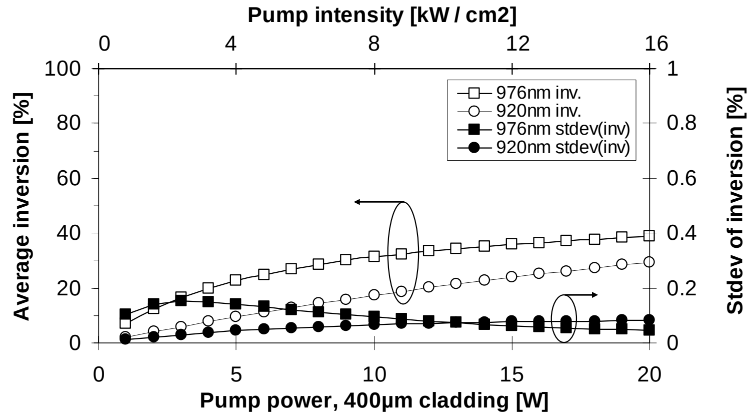

Fig. 4. Average inversion and standard deviation of the inversion vs. pump power for a cladding-pumped, Yb-doped fiber with a 20 µm core diameter and 400 µm cladding diameter. The inversion does not have a practical threshold level after which the inversion is saturated, but rather the inversion is tunable and very flat over a range of pump power. The inversion level is mainly defined by the absorption cross section and the pump power.

The differences in the inversion profiles between core- and cladding-pumped short fiber samples are significant. In the case of core pumping, the inversion profile is very flat in the beginning of the fiber, where the inversion is saturated. If the coupled pump power is insufficient to saturate the full length of the active fiber, high core doping levels lead to a sharp drop in the longitudinal inversion profile as the propagating pump is absorbed. By increasing the coupled pump power, the longitudinal inversion profile may retain a similar shape, but the saturated portion of the fiber becomes increasingly longer. In the case of cladding pumping, the longitudinal inversion profile as a function of input pump power is quite different. Even with small input pump powers, the inversion tends to be very flat throughout the fiber, and by increasing the pump power, the inversion increases evenly throughout the short sample, as shown in Fig. 2. The standard deviation of inversion over the 10 cm length of the fiber sample indicates that the inversion across the length is relatively uniform. Consequently, in the case of core pumping, the saturated inversion level is defined mainly by the ratio of the absorption and emission cross sections, and therefore the highest saturated inversion can be achieved by pumping at shorter wavelengths (e.g., 920 nm). On the other hand, in the cladding-pumped case, the pump brightness is typically lower, and the level of inversion will be defined more by the absorption cross section (e.g., at 976 nm the inversion is highest). It must be pointed out that for a reliable determination of the inversion level, both the pump wavelength and coupled pump power must be known.

3. RATE OF PHOTODARKENING

When measuring the PD rate of a fiber in a specific application, such as a cw laser or a pulsed amplifier, several parameters may vary simultaneously or be poorly constrained (inversion, temperature, irradiance, wavelength distribution, etc.). The results may thus seem contradictory if a given fiber photodarkens faster in one application than in another. Our hypothesiss, based on our experience with core-pumped PD measurements of single-mode fibers, was that the inversion level is the dominant parameter defining the initial PD rate.[13] The procedure to test our hypothesis was to provide a flat and tunable inversion level to fiber samples, and to measure the PD rate as a function of inversion level for multiple fibers. We chose the cladding-pumping method and used short sample lengths in order to have an easily tunable and flat inversion level in all of the fiber samples. We investigated two aluminosilicate, double-clad fibers with similar compositions but different Yb-doping levels (denoted Fiber #1 and Fiber #2).

3.1 Measurement setup

The initial PD rate was measured using the setup illustrated in Fig. 5. A HeNe probe laser at 633 nm was coupled to a single-mode fiber. This fiber was spliced to the single-mode input fiber of a commercially available multimode combiner (MMC), which also had several multimode input fibers for pump laser diodes. The latter were spliced to fiber-coupled pump diodes operating at a wavelength of ~920 nm. The output fiber of the MMC was double clad with a core diameter of 6 µm and a round cladding of 125 µm diameter. The test fibers were Yb-doped, double-clad fibers with a 6 µm core diameter and an octagonal inner cladding with a diameter of 125 µm; all fiber samples were 10 cm long. The test fiber was spliced to the output fiber of the MMC. The splice was recoated using a low-index polymer to minimize pump coupling losses to the fiber sample. The probe laser propagated mainly in the core of the sample, whereas the pump propagated in the cladding. The output pump and probe light were separated using dichroic filters, and an aperture was used to filter out probe laser light that propagated in the cladding, as illustrated. Both output pump power and transmitted probe power were measured with power meters throughout the experiment. No measurable decrease in pump power was observed due to the short sample length, the small core/cladding ratio of the fiber, and the relatively small PD-induced loss at the pump wavelength compared to the visible probe wavelength.

After each measurement a fresh fiber sample was spliced and recoated. Inversion levels for each sample with known pump power and wavelength were simulated using Liekki Application Designer v3.0. The cladding pumping and short sample length gave each sample a very uniform inversion, and the coupled pump power was used to tune the inversion, as shown in Fig. 6.

Initial experiments with Fiber #1 were performed without the water bath, with the fiber sample suspended in air and fixed only at both ends. Simulations indicated that the core temperature of the fiber may rise by more than 20 K, which could complicate the data interpretation if PD has a significant temperature dependence. In subsequent experiments, the sample fiber was immersed in a constant-temperature water bath; simulations indicate that this approach maintained a constant core temperature within a few degrees for our experimental conditions. Any probe light propagating in the cladding would also be effectively stripped within the water bath, as the uncoated part of the passive output fiber was in contact with the metal bottom of the bath. The transmitted pump power in this case could not be measured in real time, however, the measurements performed in air showed good agreement between the measured output pump power and the presumed coupled pump power. We repeated the Fiber #1 measurements using the water bath, and all Fiber #2 measurements employed the water bath.

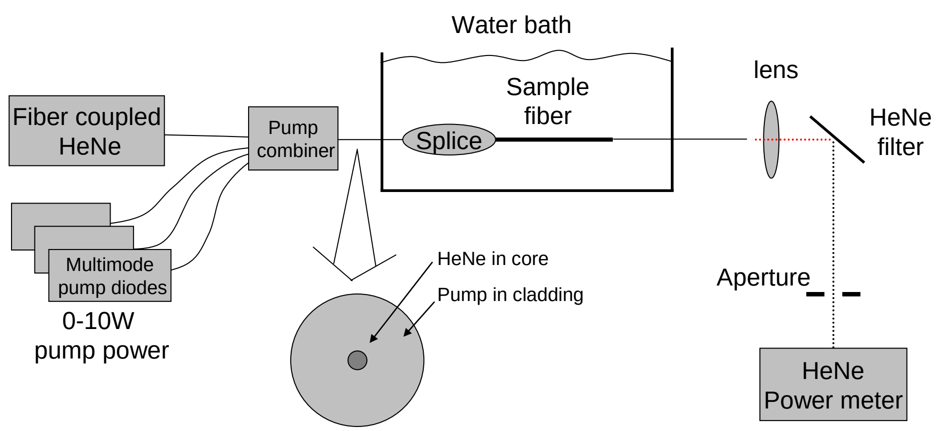

Fig. 5. Measurement setup to measure the PD rate in the Yb-doped core of the sample fiber. A longitudinally constant inversion was achieved with a short sample length, and the inversion level was tuned by varying the pump power. HeNe transmission through the core of the fiber was measured as a function of time as the fiber photodarkened.

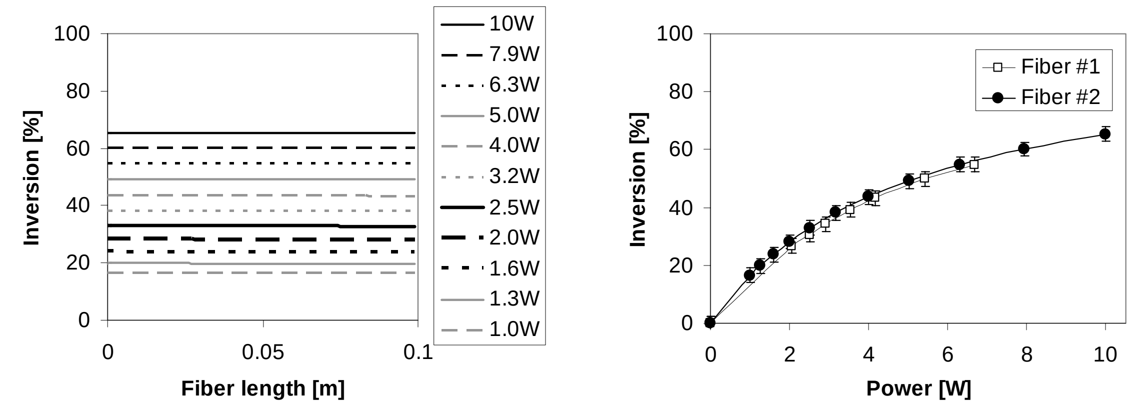

(a) (b)

Fig. 6. (a) Longitudinal inversion profile of short (10 cm) sample fibers cladding pumped using different pump powers. The induced inversion profile is spatially very flat and tunable over a wide range. (b) Simulated average inversion of fiber samples as a function of pump power.

3.2 Results

The PD rate was measured over a wide range of inversion levels, from 27% to 55% for Fiber #1 and from 30% to 63% for Fiber #2. Figure 7 shows the probe-laser transmittance as a function of time for both fibers at various inversion levels when the samples were immersed in the water bath; for Fiber #1, the results were similar when the fiber was held in the air. As seen in Fig. 7, the PD rate increased with increasing inversion. The inset in Fig. 7b shows examples of fitting results described later. The range of PD rates presented in Fig. 7 represents the dynamic range of the measurement setup. For faster PD rates, a faster detector would be required; for slower PD rates, the incident probe power would need to be monitored and the data corrected for drift in the probe-laser output power.

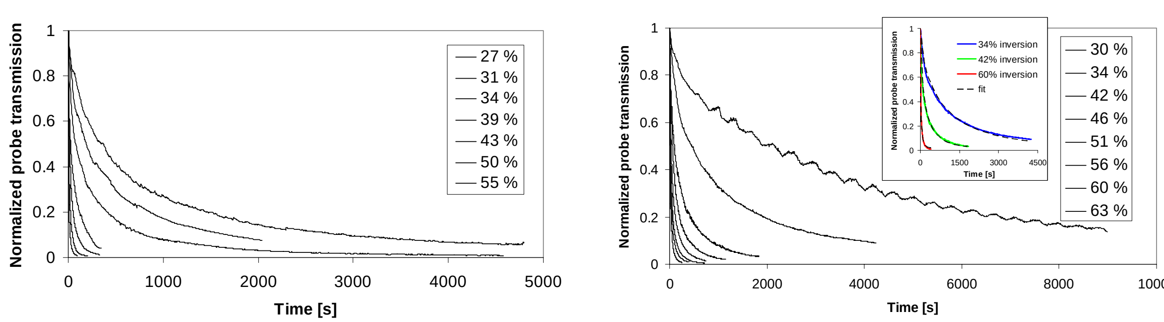

(a) (b)

Fig. 7. (a) Measurement results of Fiber #1. (b) Measurement results for Fiber #2. The probe transmission at different inversion levels are shown in the same order as indicated in the legend, lower inversion as slowest. The inset figure has examples of the fit data together with the measured data.

For each measurement, the normalized, time-dependent probe transmission (T) was fitted with a stretched exponential function[15]

$$T(t) = A\exp\left[-\left(\frac{t}{\tau}\right)^{\beta}\right] + (1 - A), \tag{1}$$

where (1-A) is the steady state transmission, β is the stretch parameter ($0 \le \beta \le 1$), t is time, and τ is the PD time constant for each measurement. The fitting was done using the least-squares method, and the parameters that gave the best agreement with the measured data were β = 0.675, and A = 0.99 for Fiber #1 and β = 0.65 and A = 0.98 for Fiber #2. Using the same fitting values for both fibers does not significantly influence the results, and the best-fit parameters were used in the fits shown in the Fig. 7b inset.

Figure 8 shows a log-log plot of the inverse of the PD time constant as a function of inversion level. The linearity of the data points indicates that the initial PD rate (the inverse of the PD time constant) is an exponential function of inversion (I), namely

$$I^n \propto \frac{1}{\tau} \Rightarrow n\log(I) \propto \log\left(\frac{1}{\tau}\right). \tag{2}$$

The slope n of the linear fit is approximately 7 for both fibers, i.e., the initial PD rate has a seventh-order dependence of the inversion level. The fiber samples were of similar aluminosilicate glass composition, however, they had different Yb concentrations. The data shown in Fig. 8 can be re-plotted as a function of the Yb excited-state number density [Yb*], which is the inversion multiplied by the Yb concentration, as shown in Fig. 9. Plotted in this manner, the results for the two fibers are identical within experimental error. This result shows that, for the glass composition of these fibers, the initial PD rate is determined exclusively by the number density of excited Yb ions, not by Yb concentration or pump level, with a seventh-order dependence on [Yb*]. We note that this conclusion is not driven by the choice of a stretched-exponential function to fit the PD data. The data can also be fit by a bi-exponential decay, and the two time constants exhibit a seventh-order dependence on [Yb*].

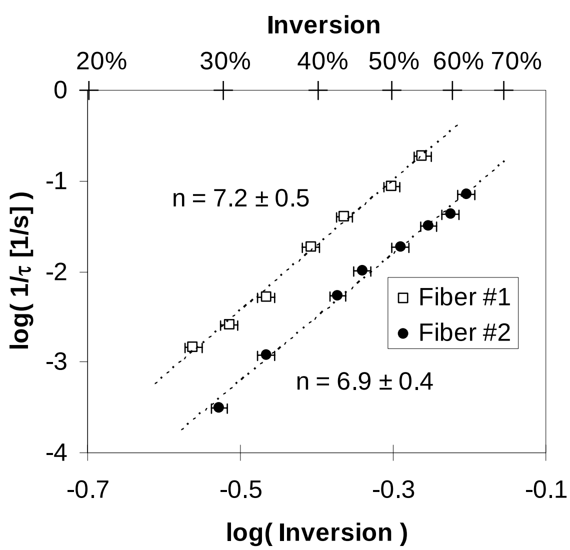

Fig. 8. Log-log plot of the inverse of the PD time constant as a function of inversion. The data for both fibers are well described by a linear fit with a slope of ~7.

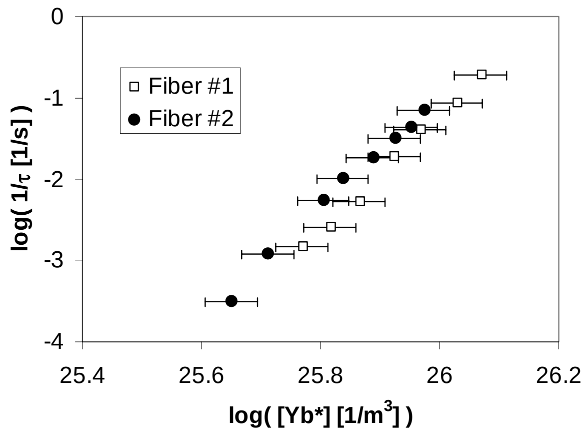

Fig. 9. The same rate data as Fig. 8 re-plotted as a function of excited-state Yb number density [Yb*]. The fibers were of similar glass composition and different Yb-ion concentration. The results suggest that the initial PD rate for a given glass composition is determined by the excited-state number density.

3.3 Discussion

The strong dependence of the initial PD rate on inversion (and excited-state Yb number density) may indicate a single, well-defined PD mechanism for the glass host of the present fibers. One possibility is the formation of color centers in the glass by photoionization. The photoionization energies for silica glasses are dependent on the dopants. Photoionization energies for sodium-doped silica glasses are reported to be as low as 5.2 eV [11], whereas pure silica has a photoionization energy of up to 8-9 eV [16]. The energy of one pump photon in these experiments was ~1.35 eV, which would give a total energy of ~9.45 eV for interaction among seven ions. The most likely energy level for a given Yb ion corresponds, however, to the emission cross-section peak at 976 nm, where the total energy would be 8.89 eV. Such energies, corresponding to single-photon wavelengths of 130-140 nm, would be enough to photoionize pure silica. It should be noted that the glass of the sample fibers was sodium free. Preliminary measurements indicate that the PD saturates following prolonged exposure to pump radiation. If saturation occurs, a mechanism to trigger the creation of a color center is required. The mechanism could be an impurity in the glass matrix or a suitably sized formation of closely packed Yb ions. If the existence of closely packed Yb ions (or clustering) is a requirement for PD, the manufacturing method of Yb-doped glass should favor homogeneous doping in order to minimize PD.[17] Additionally, due to the significant dependence of the PD rate constant on excited-state Yb number density, any local fluctuation in the Yb concentration will lead to significant differences in the initial PD rate, even if the Yb concentration averaged over a larger sample volume is constant. Although these results suggest the creation of color centers in a single, step-wise process, other physical processes cannot be ruled out. The PD mechanism may also involve sequential processes, each of which is nonlinear with pump power, for example, multiphoton excitation of sites followed by interaction of multiple sites.

Different applications of fiber sources employing a given Yb-doped fiber, for example, CW lasers, CW amplifiers, pulsed amplifiers, and Q-switched lasers, will exhibit PD degradation over a very wide range of time scales, depending on the inversion of the fiber. Presuming the seventh-order power dependence on inversion, the PD time constant for an inversion of 5% is over 500,000 times larger than for an inversion of 35%. A 5% inversion may be achieved in a CW fiber laser, whereas a 35% inversion is more likely to occur in an amplifier setup.

The PD characterization of a fiber should be performed with high inversion, and the inversion needs to be repeatable between samples in order to obtain reliable results. For example, by using high inversion, the lifetime PD potential of a CW fiber laser (low inversion) can be estimated without running the fiber for tens of thousands of hours.

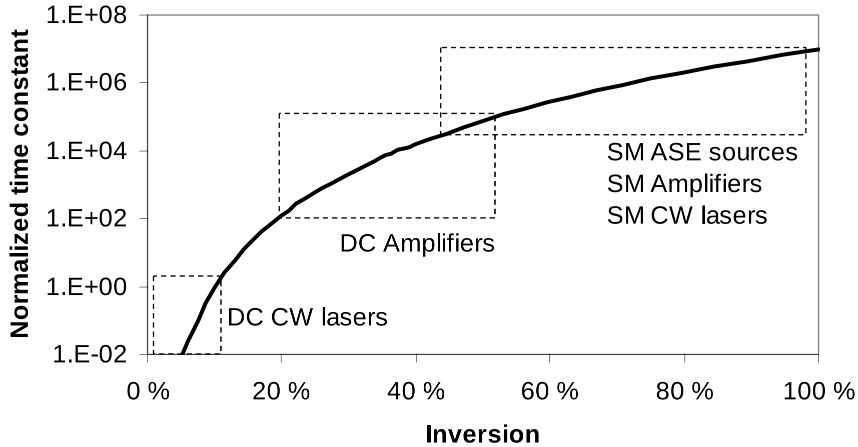

Fig. 10. The normalized initial PD time constant as a function of inversion, presuming a seventh-order dependence on inversion. Operating regimes for various applications are highlighted.

4. CONCLUSIONS

The PD rate constant in these experiments can be parameterized in terms of single variable, the excited-state Yb concentration (or inversion level) in the fiber. This result has important implications for comparison and extrapolation of PD measurements among different fibers and operating conditions. The inversion level of a fiber sample is defined by the interplay of pump intensity, pump wavelength, fiber characteristics (core size, inner-cladding size, sample length, Yb concentration) and optical feedback. Inducing inversion using a single-mode pump diode and core pumping requires sufficient pump intensity to saturate the inversion of the sample. The inversion saturation level is defined roughly by the ratio of absorption and emission cross sections at the pump wavelength; the saturated inversion with, for example, 920 nm pumping is higher than for 976 nm pumping. As the saturation threshold is exceeded, inversion is no longer pump-power dependent. In a convenient benchmarking method for LMA fibers, a stable, uniform, and repeatable inversion in a short sample fiber can be achieved using cladding pumping rather than core pumping. As the cladding-pumping method uses a lower pump intensity, the inversion of the sample is not saturated and can be varied by changing the pump power. Due to the lower pump intensity, the attainable inversion level is defined mainly by the absorption cross section at the pump wavelength and the pump power.

The time constant for PD appears to follow a simple power law and is approximately proportional to $[Yb^*]^7$, where $[Yb^*]$ is the number density of Yb ions in the excited state. This simple functional dependence for the initial PD rate may be an indication of a single, well-defined mechanism for color-center formation, although other physical processes cannot be ruled out at this stage.

The very high-order dependence on population inversion has significant implications for fiber devices. For example, if we assume the above seventh-order dependence, a fiber operating as a pulsed amplifier may photodarken up to 10^5-10^7 times faster than one used in a cw laser (even a cw laser operating at very high output power), assuming average inversions of 40-50% and 5-10%, respectively. Pulsed lasers or amplifiers that are operated with cw pumping will have a time-dependent inversion profile that is a function of pulse energy, wavelength, pulse duration, and repetition rate, making it challenging to correlate any benchmarking results to actual performance degradation of an operational system.

The present results demonstrate the importance of performing PD measurements under uniform population inversion. The seventh-order dependence on inversion level makes quantitative analysis of a fiber with non-uniform inversion very difficult. Furthermore, the time required to record the PD decay curve can be inconveniently long (or impractical) if insufficient pump power is available to achieve a high enough level of inversion.

Further experiments should be undertaken to extend this study to a wide range of fiber compositions, to explore the temperature dependence of the PD process, and to analyze the underlying photochemical mechanism(s) for such optically induced excess loss.

REFERENCES

1. D.C. Brown and H.J. Hoffman, "Thermal, stress, and thermo-optic effects in high average power double-clad silica fiber lasers," *IEEE J. Quantum Electron*. 37(2), 207-217 (2001).
2. C.-H. Liu, B. Ehlers, F. Doerfel, S. Heinemann, A. Carter, K. Tankala, J. Farroni, and A. Galvanauskas, "810W continuous-wave and single transverse-mode fibre laser using 20 µm core Yb-doped double-clad fibre," *Electron. Lett*. 40, 23 (2004).
3. R. Paschotta, J. Nilsson, A. C. Tropper, and D. C. Hanna, "Ytterbium-Doped Fiber Amplifiers," *IEEE J. Quantum Electron*. 33, 7 (1997).
4. D.A.V. Kliner, F. Di Teodoro, J.P. Koplow, S.W. Moore, and A.V. Smith, "Efficient second, third, fourth, and fifth harmonic generation of a Yb-doped fiber amplifier," *Opt. Commun*. 210, 393 (2002).
5. S. Norman, M. Zervas, A. Appleyard, M. Durkin, R. Horley, M. Varnham, J. Nilsson, and Y. Jeong, "Latest development of high power fiber lasers in SPI," in *Fiber Lasers: Technology, Systems, and Applications*, L.N. Durvasula, ed., Proc. SPIE 5335, 229-237 (2004).
6. N.S. Platonov, D.V. Gapontsev, V.P. Gapontsev, and V. Shumilin, "135W CW fiber laser with perfect single mode output," in *Conference of Lasers and Electro-Optics*, CLEO Technical Digest (OSA, 2002), paper CPDC3.
7. M. Broer, D. M. Krol, and D. J. DiGiovanni, "Highly nonlinear near-resonant photodarkening in a thulium-doped aluminosilicate glass fiber," *Opt. Lett*. 18(10), 799 (1993).
8. G. R. Atkins and A. L. G. Carter, "Photodarkening in Tb^{3+}-doped phosphosilicate and germanosilicate optical fibers," *Opt. Lett*. 19(12), 874 (1994).
9. M.M. Broer, R.L. Cone, and J.R. Sompson, "Ultraviolet-induced distributed-feedback gratings in Ce^{3+}-doped silica optical fibers," *Opt. Lett*. 16(18), 1391 (1991).
10. E.G. Behrens and R.C. Powell, "Characteristics of laser-induced gratings in Pr^{3+}- and Eu^{3+} -doped silicate glasses," *J. Opt. Soc. Am. B* 7(8), 1437 (1990).
11. L. B. Glebov, "Linear and Nonlinear Photoionization of Silicate Glasses," *Glass Sci. Technol*. 75, C2 (2002).
12. J. J. Koponen, M. J. Söderlund, H. J. Hoffman, and S. K. T. Tammela, "Measuring photodarkening from single-mode ytterbium doped silica fibers", *Opt. Express* 14(24), 11539 (2006).
13. J. J. Koponen, M. J. Söderlund, S. K. Tammela, and H. Po, "Photodarkening in ytterbium-doped silica fibers," in *Optically Based Materials and Optically Based Biological and Chemical Sensing for Defence II*, John C. Carrano, Arturas Zukauskas, Anthony W. Vere, James G. Grote, François Kajzar, Eds., Proc. SPIE 5990, 599008 (2005).
14. J. Jasapara, M. Andrejco, D. DiGiovanni, and R. Windeler, "Effect of heat and H2 gas on the photo-darkening of Yb^{+3} fibers," in *Conference of Lasers and Electro-Optics*, CLEO Technical Digest (OSA, 2006), paper CTuQ5.
15. A. Chandonnet, P. Laperle, S. LaRochelle, and R. Vallée, "Photodegradation of fluoride glass blue fiber laser," in *Photosensitive Optical Materials and Devices*, Mark P. Andrews, Ed., Proc. SPIE 2998, 70 (1997).
16. D.L. Griscom, "The electronic structure of SiO2: A review of recent spectroscopic and theoretical advances," *J. Non-Cryst. Solids* 24, 155 (1977).
17. S. Tammela, M. Söderlund, J. Koponen, V. Philippov, and P. Stenius, "The potential of direct nanoparticle deposition for the next generation active fibers," in *Optical Components and Materials III*, Michel J. Digonnet, Shibin Jiang, Eds. Proc. SPIE 6116 (2006).